Single-molecule denaturation and degradation of proteins by the AAA+ ClpXP protease

Yongdae Shin[a,1], Joseph H. Davis[b,1], Ricardo R. Brau[c,1,2], Andreas Martin[b,1,3], Jon A. Kenniston[b,4], Tania A. Baker[b,d], Robert T. Sauer[b,5], and Matthew J. Lang[a,c,5]

Departments of [a]Mechanical Engineering, [b]Biology, and [c]Biological Engineering and [d]Howard Hughes Medical Institute, Massachusetts Institute of Technology, Cambridge, MA 02139

Contributed by Robert T. Sauer, September 23, 2009 (sent for review July 14, 2009)

ClpXP is an ATP-fueled molecular machine that unfolds and degrades target proteins. ClpX, an AAA+ enzyme, recognizes specific proteins, and then uses cycles of ATP hydrolysis to denature any native structure and to translocate the unfolded polypeptide into ClpP for degradation. Here, we develop and apply single-molecule fluorescence assays to probe the kinetics of protein denaturation and degradation by ClpXP. These assays employ a single-chain variant of the ClpX hexamer, linked via a single biotin to a streptavidin-coated surface, and fusion substrates with an N-terminal fluorophore and a C-terminal GFP-titin-ssrA module. In the presence of adenosine 5′-[γ-thio]triphosphate (ATPγS), ClpXP degrades the titin-ssrA portion of these substrates but stalls when it encounters GFP. Exchange into ATP then allows synchronous resumption of denaturation and degradation of GFP and any downstream domains. GFP unfolding can be monitored directly, because intrinsic fluorescence is quenched by denaturation. The time required for complete degradation coincides with loss of the substrate fluorophore from the protease complex. Fitting single-molecule data for a set of related substrates provides time constants for ClpX unfolding, translocation, and a terminal step that may involve product release. Comparison of these single-molecule results with kinetics measured in bulk solution indicates similar levels of microscopic and macroscopic ClpXP activity. These results support a stochastic engagement/unfolding mechanism that ultimately results in highly processive degradation and set the stage for more detailed single-molecule studies of machine function.

molecular machine | protein degradation | single-molecule fluorescence | protein unfolding | protein translocation

Molecular machines of the AAA+ (ATPases associated with diverse cellular activities) enzyme superfamily play crucial roles in cellular processes ranging from protein degradation and DNA replication to membrane fusion and the movement of motor proteins along microtubule tracks (1–2). AAA+ proteases degrade proteins that are damaged, remove proteins that are no longer needed by the cell, and function in regulatory circuits that require proteolysis of specific target proteins. In bacteria, such as *Escherichia coli*, intracellular proteolysis is carried out by multiple ATP-dependent proteases, including ClpXP, ClpAP, HslUV, Lon, and FtsH (3). In the ClpXP machine, for example, the AAA+ ClpX component engages protein substrates, unfolds them, and ultimately translocates the denatured polypeptide into an internal chamber of the associated ClpP peptidase for irreversible proteolysis (4). Thus, the overall process of ClpXP degradation involves the operation and coordination of enzymatic machinery for substrate recognition, denaturation, translocation, and degradation.

ClpX functions as an asymmetric ring of six subunits, with the sites for ATP binding and hydrolysis located at subunit interfaces (5–6). ClpP is also active as a multimer, in which two stacked heptameric rings enclose a degradation chamber containing 14 active sites for peptide-bond cleavage (7). A hexameric ClpX ring and a heptameric ClpP ring stack coaxially, creating a central channel that allows translocation of unfolded substrates through the ClpX pore and into the ClpP peptidase chamber (8). ClpX recognizes specific substrates by binding to exposed peptide sequences. For example, appending the ssrA tag (AANDENYALAA) to the C terminus of a protein makes it a substrate for ClpXP degradation (9). The ssrA tag initially binds in the axial pore of ClpX (10, 11). Changes in ClpX conformation, powered by ATP binding and hydrolysis, are then postulated to initiate tag translocation through the pore. Because native proteins are larger than the ClpX pore, continued translocation eventually pulls on the attached protein and results in an unfolding force. For very stable protein domains, hundreds of cycles of ATP hydrolysis can be required on average before unfolding is successful, although single mutations that destabilize the substrate can reduce this value almost 50-fold (12). Moreover, a hyperstable substrate can dissociate from the enzyme after an unsuccessful denaturation attempt (13). Thus, any structural perturbations caused by the transient strain of attempted unfolding would almost certainly relax before that substrate was rebound by another enzyme. These facts suggest that successful unfolding results from a combination of the applied pulling force and stochastic changes in protein stability. For example, fluctuations in the distribution of thermal energy in the protein could result in occasional fraying of secondary structure or in partial unfolding that then allows a single ClpX pulling event to cooperatively denature the entire protein domain (12). It is also possible that all ClpXP enzymes in bulk solution hydrolyze ATP but only a small fraction is active in denaturation. By this model, rare encounters between "active" ClpXP and substrate could lead to efficient denaturation in a single turnover, whereas the vast majority of substrate·enzyme interactions would not. In this case, average properties calculated assuming that all ClpXP enzymes in bulk solution are equally active could be very different from the actual properties of individual enzymes.

Since the first detection of single fluorophores at cryogenic temperatures (14), single-molecule fluorescence has become a powerful technique for exploring the nanoscale behavior of individual molecules. For example, such studies have revealed important information regarding mechanoenzyme motility, un-

Author contributions: Y.S., J.H.D., R.R.B., A.M., J.A.K., T.A.B., R.T.S., and M.J.L. designed research; Y.S., J.H.D., R.R.B., A.M., and J.A.K. performed research; Y.S., J.H.D., R.R.B., and A.M. contributed new reagents/analytic tools; Y.S., J.H.D., R.R.B., A.M., J.A.K., T.A.B., R.T.S., and M.J.L. analyzed data; and Y.S., J.H.D., J.A.K., R.T.S., and M.J.L. wrote the paper.

The authors declare no conflict of interest.

Freely available online through the PNAS open access option.

[1]Y.S., J.H.D., R.R.B., and A.M. contributed equally to this work.

[2]Present address: L.E.K. Consulting, Boston, MA 02109.

[3]Present address: Department of Molecular and Cell Biology, University of California, Berkeley, CA 94720.

[4]Present address: Departments of Biochemistry and Biophysics, University of Pennsylvania, Philadelphia, PA 19104.

[5]To whom correspondence may be addressed. E-mail: mjlang@mit.edu or bobsauer@mit.edu.

This article contains supporting information online at www.pnas.org/cgi/content/full/0910484106/DCSupplemental.

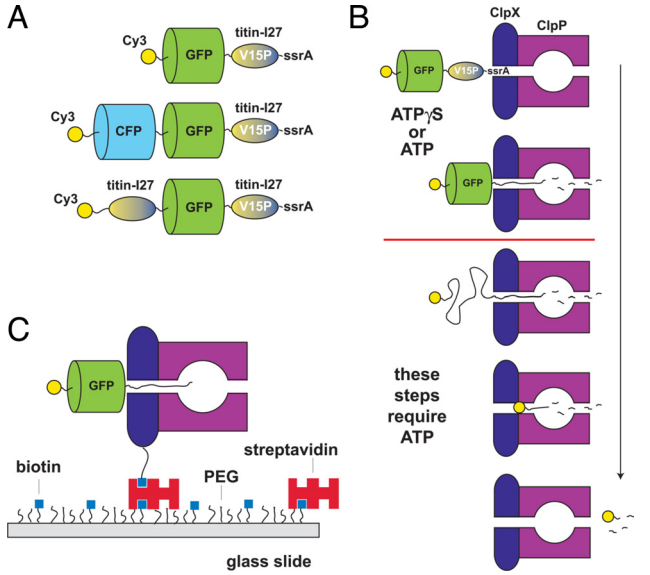

Fig. 1. Substrates and methods used for single-molecule assays of ClpXP degradation. (*A*) Substrates contained an N-terminal Cy3 fluorophore, a GFP domain, a titin-I27 domain with the V15P mutation, and a C-terminal ssrA tag. (*B*) In the presence of ATPγS, ClpXP degrades the titin^{V15P}-ssrA portion of substrates but stalls because it cannot denature GFP (21). Exchange into ATP then permits GFP denaturation and completion of degradation. (*C*) For single-molecule experiments, preengaged complexes of substrates, biotinylated ClpX^{SC}, and ClpP were formed in the presence of ATPγS, tethered to a PEG-coated glass surface via PEG-biotin·streptavidin, and visualized by TIRF microscopy. Degradation reactions were initiated by exchange of ATP for ATPγS.

assisted and chaperone-mediated protein folding, and enzyme dynamics (15–18). Here, we develop and apply a single-molecule fluorescence assay to probe the kinetics of ClpXP-mediated substrate denaturation and degradation. Our results provide important support for mechanistic conclusions based on ensemble experiments and set the stage for more detailed single-molecule studies of ClpXP function.

Results

Experimental Design. We had to overcome several problems during assay development. For example, wild-type *E. coli* ClpX bound nonspecifically and nonfunctionally to surfaces, apparently because hexamers dissociated and the isolated subunits were prone to denaturation. In addition, some methods of surface attachment precluded ClpX binding to ClpP. Eventually, we used a single-chain ClpX pseudohexamer lacking the N-domain (19), which is not needed to degrade ssrA-tagged substrates (20) but seemed to contribute to surface inactivation. This single-chain variant (ClpX^{SC}) was cloned with a sequence that allowed enzyme-mediated covalent attachment of one biotin molecule to each pseudohexamer. The biotinylated ClpX^{SC} enzyme was as active as wild-type ClpX in ClpP-mediated degradation of a GFP-ssrA substrate (see Fig. S1).

Three substrates were used for single-molecule studies (Fig. 1*A*). Each had an N-terminal cysteine, which we modified with a Cy3 fluorophore, and a common GFP-titin^{V15P}-ssrA unit, consisting of a GFP domain, the I27 domain of titin bearing the destabilizing V15P mutation, and a C-terminal ssrA tag (12, 21). In the presence of Mg^{2+} and adenosine 5′-[γ-thio]triphosphate (ATPγS), an ATP analog, which ClpX hydrolyzes slowly, ClpXP degrades the titin^{V15P}-ssrA portion of these substrates but stalls when it reaches the GFP domain (21; Fig. 1*B*). These stalled complexes are stable after chelation of Mg^{2+} by excess EDTA, which prevents nucleoside-triphosphate hydrolysis, and after replacing ATPγS/EDTA with ATP/EDTA (see Fig. S2). Subsequent addition of ATP/Mg^{2+} then initiates ATP hydrolysis and degradation of the GFP domain and downstream portions of the substrate (21). Substrates were incubated with biotinylated ClpX^{SC}, ClpP, and ATPγS/Mg^{2+} to form stalled complexes, which were then introduced into a flow cell, immobilized on a glass slide coated with a mixture of covalently attached PEG and PEG-biotin·streptavidin (22), and quantified by objective-side TIRF imaging (Fig. 1*C*). We included an oxygen scavenging system (15) and minimized the intensity and/or duration of laser excitation to reduce photobleaching. The Cy3 dye served as a marker for stalled complexes and remained bound to the surface-attached enzyme until completion of degradation.

Initial controls were performed by using the Cy3-GFP-titin^{V15P}-ssrA substrate. Under standard conditions with biotinylated ClpX^{SC}, ClpP, and ATPγS/Mg^{2+}, we observed 99.8 ± 7.2 fluorescent spots per field of view (Fig. 2*A*). Several experiments established that most spots corresponded to complexes of the substrate and the immobilized protease. (*i*) When biotinylated ClpX^{SC} was omitted (Fig. 2*B*) or nonbiotinylated ClpX^{SC} was used, 9 ± 2 spots were observed. (*ii*) When ATPγS (Fig. 2*C*) or Mg^{2+} was omitted from the preincubation, 13 ± 3 spots were observed. (*iii*) When Cy3-labeled substrate was omitted, no more than two spots were observed. (*iv*) In the continual presence of ATPγS/Mg^{2+}, Cy3-labeled substrate photobleached in an exponential process with a time constant of 330 s (see Fig. S3*A*), similar to the photobleaching times of Cy3-labeled molecules bound to control surfaces. (*v*) When buffer with Mg^{2+} but no nucleotide was flowed over the surface, most spots disappeared with a time constant of ≈14 s (see Fig. S3*B*), consistent with studies showing that nucleotide is required for ClpX to maintain an active grip on the substrate (11).

Single-Molecule Degradation/Denaturation. After exchanging ATP for ATPγS in the absence of Mg^{2+}, we excited the Cy3 dye,

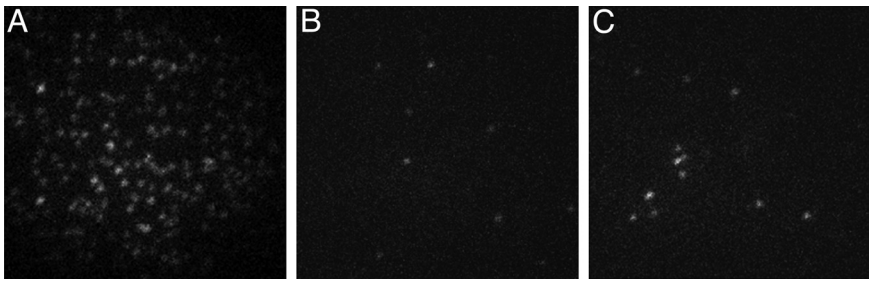

Fig. 2. Single-molecule TIRF images of the Cy3-GFP-titin^{V15P}-ssrA substrate bound to a glass surface coated with PEG and PEG-biotin·streptavidin. (*A*) Approximately 100 fluorescent spots were detected after preincubation of the substrate (1 μM) with biotinylated ClpX^{SC} (0.31 μM) ClpP (1 μM), ATPγS (2 mM), and Mg^{2+} (10 mM), and the mixture was flowed over the surface. Far fewer spots were detected when biotinylated ClpX^{SC} (*B*) or ATPγS (*C*) was omitted from the preincubation mix.

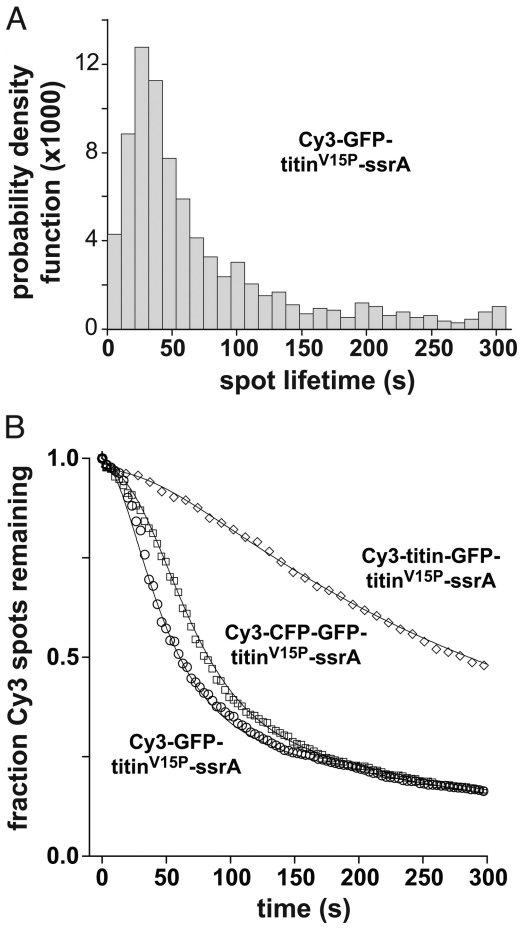

Fig. 3. Single-molecule degradation. (*A*) Distribution of spot lifetimes for the Cy3-GFP-titin^{V15P}-ssrA substrate. (*B*) Kinetic profiles of single-molecule ClpXP degradation were constructed by summing the number of Cy3 spots in TIRF images taken at 3- to 9-s intervals after initiating degradation at ≈18 °C by addition of ATP/Mg^{2+} and normalizing to the initial value. The total number of initial spots was 1,122 for the Cy3-GFP-titin^{V15P}-ssrA substrate, 974 for the Cy3-CFP-GFP-titin^{V15P}-ssrA substrate, and 419 for the Cy3-titin-GFP-titin^{V15P}-ssrA substrate. The solid lines are fits to reaction models described in *Kinetic Modeling*.

focused, and selected a field of view containing immobilized complexes of ClpX^{SC}·ClpP and the preengaged Cy3-GFP-titin^{V15P}-ssrA substrate. ATP/Mg^{2+} was then injected into the flow cell to initiate unfolding and degradation. Images were acquired at intervals (typically 3–5 s), and a custom software algorithm was used to quantify the lifetime of each spot. These data were combined for a large number of spots (1,122 spots) observed in 11 independent experiments and are presented as a probability density distribution of spot lifetimes (Fig. 3*A*) or as fractional spot populations as a function of time (Fig. 3*B*). As discussed below, these data can be corrected for photobleaching and related to the time required by the immobilized protease to unfold, translocate, and degrade substrates.

After addition of ATP/Mg^{2+} (1/10 mM), the population of the preengaged Cy3-GFP-titin^{V15P}-ssrA substrate decreased to half the initial value in ≈60 s (Fig. 3*B*). Several results indicated that the majority of this population decrease represents active ClpXP degradation. First, spot loss was faster with ATP/Mg^{2+} than with ATPγS/Mg^{2+} (50% loss in 231 s). In the latter experiment, degradation does not occur, and spots are only lost via photobleaching. Second, as expected from solution experiments (21), spot loss slowed when a lower concentration of ATP (0.1 mM) was used (50% loss in 90 s; see Fig. S4*A*) or when a mixture of ATP/ATPγS (1/0.25 mM) was used (50% loss in 155 s; see Fig. S4*B*).

We used substrates with additional domains to confirm that the loss of Cy3 fluorescence correlated with the time required for complete ClpXP degradation. For example, single-molecule ClpXP degradation of both Cy3-CFP-GFP-titin^{V15P}-ssrA (50% loss in 80 s) and Cy3-titin-GFP-titin^{V15P}-ssrA (50% loss in 279 s)* proceeded more slowly than degradation of Cy3-GFP-titin^{V15P}-ssrA (Fig. 3*B*). The relative rates of single-molecule ClpXP degradation of all three substrates were consistent with solution studies (12, 21), in which GFP and CFP domains are degraded at similar rates, but titin is degraded ≈4-fold more slowly because of its exceptional mechanical stability. These results are also consistent with studies that show that degradation of ssrA-tagged substrates proceeds processively from the C to the N terminus (23, 13), and thus the Cy3 dye is lost only when degradation is complete.

The processive model predicts that GFP denaturation should be an early event in overall degradation (Fig. 1*B*). To test this hypothesis, we monitored loss of fluorescent GFP spots after initiating ClpXP denaturation of preengaged GFP-titin^{V15P}-ssrA. As expected, GFP spots were lost at a faster rate than Cy3 spots (Fig. 4*A*), indicating that denaturation of the GFP domain occurs earlier than release of the Cy3 fluorophore during ClpXP degradation. Fitting of the GFP data, including a correction for photobleaching, gave a time constant of 19 s for denaturation of this domain.

Kinetic Modeling. We globally fit the degradation data for Cy3-GFP-titin^{V15P}-ssrA (called S1) and Cy3-CFP-GFP-titin^{V15P}-ssrA (called S2) to kinetic models with individual steps for unfolding (τ_{unf}) and translocation (τ_{trans}) of each domain (see *Materials and Methods*). Solution studies indicate that ClpXP unfolds and translocates GFP and CFP at similar rates (21), and thus we used the same time constants for both domains. A model including just these kinetic steps predicts that S2 should take twice as long to degrade as S1 and fit the data poorly. Indeed, S2 was only degraded ≈1.5-fold more slowly than S1 in our experiments, suggesting that an extra slow step contributes to both reactions. Fitting to the following reactions, which include a time constant (τ_{term}) for an unspecified terminal step, resulted in good simultaneous fits to both data sets (Fig. 3*B*).

$$\mathrm{S1} \xrightarrow{\tau_{unf}} \mathrm{I1} \xrightarrow{\tau_{trans}} \mathrm{I2} \xrightarrow{\tau_{term}} \text{degraded}$$

$$\mathrm{S2} \xrightarrow{\tau_{unf}} \mathrm{I1} \xrightarrow{\tau_{trans}} \mathrm{I2} \xrightarrow{\tau_{unf}} \mathrm{I3} \xrightarrow{\tau_{trans}} \mathrm{I4} \xrightarrow{\tau_{term}} \text{degraded.}$$

When unfolding was constrained to the experimental value (τ_{unf} = 19 s), the fitted time constants were τ_{trans} = 6.2 s and τ_{term} = 29.6 s, yielding time constants for overall degradation of 54.8 s for S1 and 80 s for S2 (Table S1).

We also fit the data for Cy3-titin-GFP-titin^{V15P}-ssrA degradation by using the τ_{unf} and τ_{trans} values determined for GFP, assuming that τ_{trans} for the titin domain was half the GFP value because it has half as many amino acids, allowing τ_{unf} for titin to vary, and using the τ_{term} value obtained above. This procedure gave a good fit of the experimental data (Fig. 3*B*) with a time constant of 347 s for titin unfolding (Table S1), indicating that ClpXP unfolding of the titin domain proceeds almost 20-fold more slowly than unfolding of the GFP or CFP domains.

*For this substrate, a 9-s interval between images was used, and the photobleaching time constant was 1,330 s.

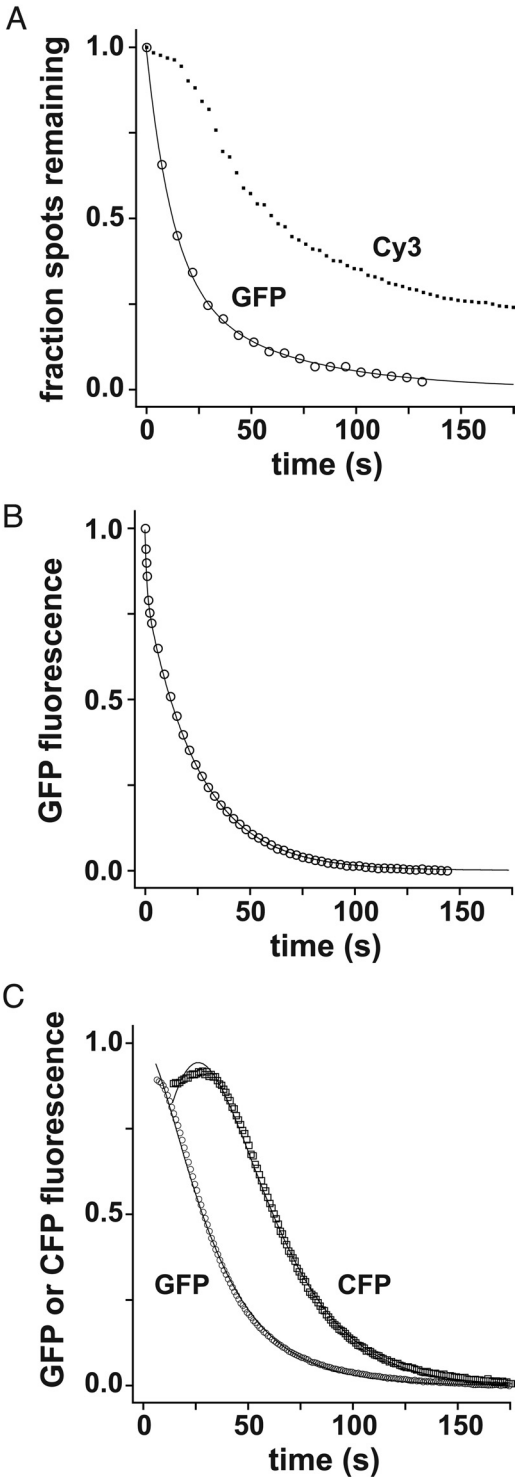

Fig. 4. Substrate denaturation assayed by single-molecule or solution experiments. (*A*) Single-molecule ClpXP denaturation of the preengaged Cy3-GFP-titin^{V15P}-ssrA substrate. Circles represent a kinetic profile constructed by summing the number of GFP spots in TIRF images taken at 7-s intervals after addition of ATP/Mg^{2+} and normalizing to the initial value (251 spots). The solid line is a double exponential fit [$y = 0.9{\cdot}\exp(-t/17.3) + 0.1{\cdot}\exp(-t/197)$]. After correcting the time constant for the dominant phase to account for a photobleaching contribution, the time constant for GFP denaturation was 19 s. The squares show the Cy3 degradation data for the same substrate. (*B*) Solution denaturation. Preengaged complexes of Cy3-GFP-titin^{V15P}-ssrA, ClpX^{SC}, and ClpP were generated in the presence of ATPγS/Mg^{2+}, purified, and GFP denaturation at 18 °C was initiated by addition of ATP/Mg^{2+} in a stopped-flow instrument and monitored by changes in GFP fluorescence (20). The solid line is a double exponential fit of the data [$y = 0.19{\cdot}\exp(-t/0.87) + 0.81{\cdot}\exp(-t/25)$]. The fast phase may represent diminished fluorescence caused by ClpX extraction of the C-terminal β-strand of GFP (see ref. 21). (*C*) Solution denaturation of the CFP-GFP-titin^{CM}-ssrA substrate. At time 0, the substrate (0.5 μM) was mixed with ClpX^{SC} (1 μM), ClpP (2 μM), the SspB adaptor (0.75 μM), and an ATP regeneration system at 18 °C. Changes in GFP fluorescence or CFP fluorescence were monitored in separate experiments. The solid lines are fits to the model described in *Substrate Unfolding and Translocation in Solution*.

Substrate Unfolding and Translocation in Solution. The single-molecule experiments were performed at ≈18 °C, a temperature where ClpXP activity is not typically assayed. To allow comparisons, we performed a set of bulk experiments in solution at 18 °C. Because some experiments required initial ClpXP binding and degradation of the titin^{V15P}-ssrA portion of substrates, we unfolded the titin^{V15P} domain by carboxymethylation (titin^{CM}) to preclude the need for unfolding (12). First, we determined K_M (1.9 μM) and V_{max} (0.62 min^{-1}) for degradation of GFP-titin^{CM}-ssrA by biotinylated ClpX^{SC} and ClpP. The corresponding time constant for steady-state degradation (97 s) was longer than for single-molecule degradation but includes the times required for binding, engagement, and translocation of titin^{CM} as well as for denaturation and translocation of GFP.

To study the GFP-unfolding reaction alone, we purified preengaged complexes of GFP-titin^{V15P}-ssrA with ClpX^{SC}·ClpP and initiated degradation by stopped-flow addition of ATP/Mg^{2+} (21). In this experiment, the loss of native GFP fluorescence, which accompanied ClpX-mediated unfolding, showed a minor burst phase (amplitude 19%; τ = 0.87 s) and a major unfolding phase (amplitude 81%; τ = 25 s) (Fig. 4*B*). Importantly, the kinetics of GFP unfolding in this solution experiment were similar to the kinetics estimated from the single-molecule data (τ = 19 s). Given the lack of precise temperature control and low time resolution in the single-molecule experiments, the differences between these values are probably not significant.

Finally, we monitored loss of GFP or CFP fluorescence under single-turnover conditions with ClpXP in 2-fold excess over CFP-GFP-titin^{CM}-ssrA (Fig. 4*C*). In these experiments, ClpXP must bind, engage, and translocate the unfolded titin^{CM}-ssrA portion of the substrate and then denature/translocate the GFP domain followed by the CFP domain. Fitting the GFP data gave a time constant of 10 s for binding/engagement/translocation of titin^{CM}-ssrA and a time constant of 25 s for GFP denaturation, the same value determined above using the preengaged substrate (Fig. 4*C*). The CFP data fit well to a model with time constants of 10 s for titin^{CM}-ssrA binding/engagement/translocation, 20 s for GFP unfolding, 6 s for translocation of unfolded GFP, and 20 s for CFP unfolding (Fig. 4*C*). The difference in the GFP unfolding value for the two fits is probably caused by poor fitting of the initial rise in fluorescence that occurs in the CFP trace because of the loss of FRET that occurs upon GFP denaturation (Fig. 4*C*). Nevertheless, the kinetic constants obtained from these solution experiments were very similar to the values obtained by fitting the single-molecule data.

Discussion

In our experiments, individual complexes of surface-attached ClpXP enzymes with preengaged substrates containing a Cy3 fluorophore are detected by TIRF microscopy. Under appropriate experimental conditions, these complexes remain fluorescent until the Cy3 dye is removed by the final steps of the degradation reaction or is photobleached. The photobleaching rate can be independently determined, allowing pooled population data to be fitted to determine apparent rates of single-molecule degradation. Multiple experiments indicate that these rates reflect degradation of the complete substrate. First, single-

molecule degradation times increased as additional domains were added to the substrate and as these extra domains became more difficult to denature. Second, ClpXP degraded the same substrate more slowly when lower concentrations of ATP or mixtures of ATP/ATPγS were used, as expected from solution studies (21). Third, monitoring GFP instead of Cy3 fluorescence during degradation of GFP-titin^{V15P}-ssrA resulted in faster rates. This result is expected because GFP fluorescence is immediately quenched upon ClpX-mediated denaturation, whereas loss of Cy3 requires additional kinetic steps, including translocation of the unfolded GFP polypeptide, proteolysis by ClpP, and product release. These combined results also provide strong support for a model in which ClpXP degradation of ssrA-tagged substrates proceeds processively from the C terminus to the N terminus (13, 21, 23).

In our single-molecule experiments, most ClpXP enzymes that engaged the substrate in the presence of ATPγS were then able to denature GFP and to complete the degradation reaction when ATP was added. For example, when we monitored single-molecule GFP denaturation, 90% of the fluorescence loss occurred by the denaturation pathway with 10% following a photobleaching-only pathway. This ratio is almost exactly that predicted from control experiments, in which ≈10% of the Cy3-GFP-titin^{V15P}-ssrA substrate appeared to be bound non-specifically to the surface. Moreover, single-molecule experiments and single-turnover solution experiments gave similar time constants for GFP denaturation and, in both cases, the data were fit reasonably well by a single exponential process. These results would not be expected if the individual enzymes in the preparations used for these studies displayed a broad range of denaturation activities, although there could be a population of completely inactive enzymes. Lower estimates of the percentage of active ClpXP enzymes (58–75%) were obtained by fitting the single-molecule degradation data. Because the overall time of laser irradiation was longer in the degradation experiments, some enzyme inactivation may occur during the experiment, potentially as a consequence of oxidative damage.

Intriguingly, good fits to our single-molecule degradation data required a step in addition to substrate denaturation and translocation. In principle, this step could correspond to slow ClpP cleavage of some polypeptide sequences, to slow product release of the Cy3-labeled peptide from ClpP, or if the final step of translocation is slow because the substrate is no longer engaged efficiently by the translocation machinery. Solution studies have shown that steady-state rates of ClpXP degradation at substrate saturation (V_{max}) are slower than those predicted from single-turnover measurements of substrate denaturation and translocation (21). Thus, the additional kinetic step suggested by our single-molecule experiments may also slow the steady-state rate of ClpXP substrate degradation in solution. It is also possible that inactive enzymes in our ClpXP preparations reduce the average activity and lead to an underestimate of V_{max}, which is calculated with the assumption that all enzymes are active. We note, however, that ClpXP degraded carboxymethylated GFP-titin^{V15P}-ssrA at a steady-state maximal rate that corresponds to a time constant of 97 s for solution degradation. The time constant for single-molecule ClpXP degradation of the GFP portion of this substrate was 55 s. The ratio of these values suggests that at least 57% of the ClpXP enzymes in solution are active. However, this value is likely to be higher because the solution reaction includes additional steps of substrate binding and translocation of the unfolded titin portion of the substrate compared to the single-molecule reaction. Importantly, these results are inconsistent with models in which the solution activity of ClpXP is mediated by a small fraction of active enzymes.

Understanding the operating principles and detailed mechanisms of complex macromolecular machines, like ClpXP, will ultimately require a combination of structural, biochemical, and biophysical approaches. Here, we have developed methods that allow a single-chain variant of ClpX to be tethered to a surface, to bind ClpP, and to carry out denaturation and degradation of specific substrate proteins. Importantly, the summed single-molecule activities of our surface-tethered ClpXP enzymes recapitulate those of a population of free enzymes in bulk single-turnover experiments. It should be straightforward to extend these methods to allow single-molecule measurements of the forces exerted during protein denaturation and/or translocation by ClpXP, to measure detailed rates and step sizes for polypeptide translocation by ClpXP, to perform multiple-color experiments, and to introduce FRET probes that will allow real-time assays of the repetitive ATP-fueled conformational changes that drive the mechanical operations of the ClpXP machine.

Materials and Methods

Protein Expression and Purification. Detailed methods for the expression and purification of enzymes and substrates are provided in *SI Text*. Before labeling substrates with Cy3 maleimide (GE Healthcare), DTT was removed by exchange into 25 mM Hepes (pH 7.2), 50 mM KCl, 1 mM EDTA, 10% glycerol. An aliquot of Cy3 maleimide (2 μL of a freshly prepared 3 mM solution in dimethyl formamide) was then added to 100 μL of the substrate solution (typically 1–5 μM), and the mixture was incubated overnight at room temperature. Unreacted Cy3 dye was removed by chromatography by using three sequential desalting columns. Controls showed that Cy3 labeling was reduced to 6% when substrates lacked a cysteine at the N terminus (see Fig. S5).

Flow Cells. Flow cells (30 × 5 mm) had a volume of ≈15 μL and were made from double-sided sticky tape gaskets sandwiched between a predrilled glass slide and an etched-glass coverslip coated with a mixture of 99% PEG (molecular weight 5,000) and 1% biotin-PEG (Laysan Bio) to minimize nonspecific binding. The holes in the drilled slide were attached to flexible tubing to allow rapid buffer exchange while minimizing motion of the sample. The flow chamber and tubing were sealed with epoxy. Preengaged substrate–enzyme complexes were formed by incubating substrates (1 μM) with single-chain ClpX^{SC} (0. 31 μM), ClpP-H$_6$ (1 μM), and ATPγS (2 mM) for 45 min in PD buffer [25 mM Hepes (pH 7.6), 100 mM KCl, 10 mM $MgCl_2$, 10% glycerol (vol/vol), 0.1% Tween-20 (vol/vol)] at 30 °C (20). After treating the flow cell with 20 μL of 0.01 mg/mL streptavidin, preengaged substrate-ClpXP complexes were diluted ≈30-fold, introduced into the flow cell, and incubated for 20 min at room temperature to allow binding of biotinylated ClpX^{SC} to the streptavidin·biotin-PEG surface. In all subsequent washes, ClpP-H$_6$ (800 nM) was included to ensure maintenance of the ClpX^{SC}·ClpP complex. After the binding step, the flow cell was washed with 2 mM ATPγS and 50 mM EDTA to chelate Mg^{2+} and prevent further hydrolysis. The chamber was then washed with PD buffer (without Mg^{2+}) plus 6 mM EDTA and 1 mM ATP. After identifying a suitable region of the surface for analysis, the shutters were closed and the stage was moved slightly to a nearby field of view. The shutters were reopened to acquire the first image and 100 μL of PD buffer plus ATP was flowed into the cell to initiate the reaction (final ATP/Mg^{2+} concentration normally 1/10 mM). An oxygen scavenging system consisting of 0.8% D(+)-glucose, 165 units/mL glucose oxidase, 2,170 units/mL catalase, and 0.1% 2-mercaptoethanol was added in this final buffer to minimize photobleaching (15).

Single-Molecule Fluorescence. Single-molecule assays were performed by using a heavily modified inverted microscope outfitted with objective-side total internal reflection fluorescence capabilities (24–25). To minimize photobleaching, the excitation laser (532 nm for Cy3; 488 nm for GFP) was modulated with an acousto-optic modulator and also rapidly toggled with an electronic shutter to extend fluorophore longevity and synchronize image acquisition. The custom TIRF system included a 1.45 N.A. 100× objective and a dichroic mirror. Images were acquired by using an EMCCD camera, which was triggered externally to collect during the 300-ms on-time of the excitation laser, with an average power of 50 μW at the specimen plane. A series of 100 images was taken at 3- to 9-s intervals for degradation experiments; 21 images were taken at 7-s intervals for the denaturation experiment. The excitation zone was typically 300 μm^2 and an average of 99.8 ± 7.2 spots were observed. Images were analyzed to determine the longevity of each fluorescent spot by using custom MATLAB software. Fig. S6 shows typical kinetic traces for Cy3 spots, in which fluorescence was lost in a single step. Blinking was observed for

some GFP spots (see Fig. S7), but the software counted only events in which fluorescence was permanently lost as degradation or photobleaching.

Solution Assays. Solution unfolding or single-turnover degradation of substrates by $ClpX^{SC}$·ClpP was measured at 18 °C by using methods previously described (21). Assays were performed in PD-1 buffer (25 mM Hepes (pH 7.6), 5 mM $MgCl_2$, 10% glycerol, and 200 mM KCl) by using a creatine-phosphate based ATP-regeneration system. GFP fluorescence (excitation 467 nm; emission 511) or CFP fluorescence (excitation 433 nm; emission 475 nm) were used to monitor unfolding. The GFP-titin^{V15P}-ssrA substrate was preengaged by using ATPγS, and the enzyme·substrate complex was exchanged into a buffer with ATP but no Mg^{2+} as described (21). GFP unfolding was initiated by mixing one volume of the preengaged enzyme·substrate complex with an equal volume of 2× ATP buffer (8 mM ATP, 32 mM creatine phosphate, and 0.64 mg/mL creatine kinase in PD buffer), and the reaction was monitored by fluorescence by using an Applied Photophysics DX.17MV stopped-flow fluorimeter equipped with a 495-nm cutoff emission filter.

Kinetic Fitting. Fitting of experimental data to kinetic models was performed by an iterative nonlinear least-squares algorithm implemented in IGOR PRO 4.07 (WaveMetrics). The probabilities for each kinetic state were derived by solving rate equations with the Laplace transform. In these models (see *SI Text* for more detail), each state either moved on to next state (e.g., from domain unfolding to translocation) or photobleached. The model also included a substrate subpopulation that only lost fluorescence by the photobleaching pathway. The sum of all probabilities except for the final nonfluorescent states corresponds to the expected fractional spot population at any given time. The experimental fractional spot populations for degradation of the S1 and S2 substrates were globally fitted to these models, after fixing the unfolding time constant of GFP (19 s) and the photobleaching time constant of Cy3 (330 s) based on independent measurements.

ACKNOWLEDGMENTS. We thank M. Aubin-Tam, C. Castro, J. Damon, A. Khalil, H. Lee, S. Moore, E. Oakes, and A. Olivares for materials, advice, and helpful discussions. T.A.B. is an employee of the Howard Hughes Medical Institute. This work was supported by National Science Foundation Career Award 0643745, a Samsung Scholarship from the Samsung Foundation of Culture, National Institutes of Health Grant AI-15706, and the Howard Hughes Medical Institute.

1. Ogura T, Wilkinson AJ (2001) AAA+ superfamily ATPases: Common structure–diverse function. *Genes Cells* 6:575–597.
2. Hanson PI, Whiteheart SW (2005) AAA+ proteins: Have engine, will work. *Nat Rev Mol Cell Biol* 6:519–529.
3. Gottesman S (2003) Proteolysis in bacterial regulatory circuits. *Annu Rev Cell Dev Biol* 19:565–587.
4. Sauer RT, et al. (2004) Sculpting the proteome with AAA+ proteases and disassembly machines. *Cell* 119:9–18.
5. Kim DY, Kim KK (2003) Crystal structure of ClpX molecular chaperone from *Helicobacter pylori*. *J Biol Chem* 278:50664–50670.
6. Glynn SE, Martin A, Nager AR, Baker TA, Sauer, RT (2009) Crystal structures of asymmetric ClpX hexamers reveal nucleotide-dependent motions in a AAA+ protein-unfolding machine. *Cell*, in press.
7. Wang J, Hartling JA, Flanagan JM (1997) The structure of ClpP at 2.3Å resolution suggests a model for ATP-dependent proteolysis. *Cell* 91:447–456.
8. Ortega J, Singh SK, Ishikawa T, Maurizi MR, Steven AC (2000) Visualization of substrate binding and translocation by the ATP-dependent protease, ClpXP. *Mol Cell* 6:1515–1521.
9. Gottesman S, Roche E, Zhou YN, Sauer RT (1998) The ClpXP and ClpAP proteases degrade proteins with C-terminal peptide tails added by the SsrA tagging system. *Genes Dev* 12:1338–1347.
10. Siddiqui SM, Sauer RT, Baker TA (2004) Role of the protein-processing pore of ClpX, an AAA+ ATPase, in recognition and engagement of specific protein substrates. *Genes Dev* 18:369–374.
11. Martin A, Baker TA, Sauer RT (2008) Pore loops of the AAA+ ClpX machine grip substrates to drive translocation and unfolding. *Nat Struct Mol Biol* 15:1147–1151.
12. Kenniston JA, Baker TA, Fernandez JM, Sauer RT (2003) Linkage between ATP consumption and mechanical unfolding during the protein processing reactions of an AAA+ degradation machine. *Cell* 114:511–520.
13. Kenniston JA, Baker TA, Sauer RT (2005) Partitioning between unfolding and release of native domains during ClpXP degradation determines substrate selectivity and partial processing. *Proc Natl Acad Sci USA* 102:1390–1395.
14. Moerner WE, Kador L (1989) Optical detection and spectroscopy of single molecules in a solid. *Phys Rev Lett* 62:2535–2538.
15. Yildiz A, et al. (2003) Myosin V walks hand-over-hand: Single fluorophore imaging with 1.5-nm localization. *Science* 300:2061–2065.
16. Deniz AA, et al. (2000) Single-molecule protein folding: Diffusion fluorescence resonance energy transfer studies of the denaturation of chymotrypsin inhibitor 2. *Proc Natl Acad Sci USA* 97:5179–5184.
17. Lu HP, Xun L, Xie XS (1998) Single-molecule enzymatic dynamics. *Science* 282:1877–1882.
18. Ueno T, Taguchi H, Tadakuma H, Yoshida M, Funatsu T (2004) GroEL mediates protein folding with a two successive timer mechanism. *Mol Cell* 14:423–434.
19. Martin A, Baker TA, Sauer RT (2005) Rebuilt AAA+ motors reveal operating principles for ATP-fuelled machines. *Nature* 437:1115–1120.
20. Singh SK, et al. (2001) Functional domains of the ClpA and ClpX molecular chaperones identified by limited proteolysis and deletion analysis. *J Biol Chem* 276:29420–29429.
21. Martin A, Baker TA, Sauer RT (2008) Protein unfolding by a AAA+ protease is dependent on ATP-hydrolysis rates and substrate energy landscapes. *Nat Struct Mol Biol* 15:139–145.
22. Joo C, et al. (2006) Real-time observation of RecA filament dynamics with single monomer resolution. *Cell* 126:515–527.
23. Lee C, Schwartz MP, Prakash S, Iwakura M, Matouschek A (2001) ATP-dependent proteases degrade their substrates by processively unraveling them from the degradation signal. *Mol Cell* 7:627–637.
24. Brau RR, Tarsa PB, Ferrer JM, Lee P, Lang MJ (2006) Interlaced optical force-fluorescence measurements for single molecule biophysics. *Biophys J* 91:1069–1077.
25. Tarsa PB, et al. (2007) Detecting force-induced molecular transitions with fluorescence resonant energy transfer. *Angew Chem Int Ed Engl* 46:1999–2001.